Identification of Informative Frequency Components of Video Path Electromagnetic Emanations for Visual Data Leakage Protection

Dilmurod Davronbekov[1], Khojiakbar Foziljonov[2], Makhbubakhon Sultonova[1], Kamola Dadamatova[2] and Amir Mukhamedzhanov[3]
[1]*Department of Technologies of Mobile Communication, Tashkent University of Information Technologies named after Muhammad al-Khwarizmi, Amir Temur Ave. 108, 100084 Tashkent, Uzbekistan*
[2]*Department of Electronics and Radiotechnics, Tashkent University of Information Technologies named after Muhammad al-Khwarizmi, Amir Temur Ave. 108, 100084 Tashkent, Uzbekistan*
[3]*Department of Software Engineering, Kazan Federal University, Kremlevskaya Str. 18, 420008 Kazan, Russia*
d.davronbekov@gmail.com, foziljonov.x.i@gmail.com, maxbubasultonova1473@gmail.com, k.dadamatova@tuit.uz, AmIMukhamedzhanov@kpfu.ru

Keywords: Compromising Electromagnetic Emanations, Video Path, Pixel Clock Harmonics, Frequency Analysis, Image Reconstruction, Software-Defined Radio, Information Leakage Protection, Electromagnetic Security.

Abstract: This paper examines the problem of visual information leakage through compromising electromagnetic emanations (CEE) from video paths of computing systems. It is shown that image reconstruction significantly depends on the distribution of informative spectral components of the CEE and their relationship to harmonics of the video signal's clock (pixel) signal. This study aims to identify frequency components at which visual information recovery is possible, as well as frequencies within which image reconstruction is difficult or impossible. The methodological basis of the study includes experimental frequency analysis of the CEE using a software-defined radio receiver and specialized software. During the experiment, multiple harmonics of the clock frequency are calculated, emission levels are measured at the corresponding frequency points, and image reconstruction is performed based on the recorded spectral components. The results show that the informative components of the CEE are unevenly distributed across the spectrum and are concentrated primarily at specific harmonic frequencies, where stable recovery of visual information is ensured. The practical significance of this work lies in the substantiation of the possibility of using selective protection methods aimed at suppressing the most vulnerable frequency components, which allows for increasing the effectiveness of preventing visual data leakage while reducing excess electromagnetic influence and maintaining the operability of computing systems.

1 INTRODUCTION

Modern computing systems increasingly serve as a primary medium for handling and displaying sensitive digital information about objects and processes, regardless of the field of human activity, is represented digitally and processed using computer systems. Information displayed on a monitor screen is transmitted from the system unit via digital interfaces (DVI, HDMI, DisplayPort) to the display device (monitor). These components together form the computer system's video path.

During the operation of computer equipment (CE) equipped with information visualization devices, CEE is emitted into the surrounding space [1]-[4]. CEE is generated in video path elements and can be intercepted over significant distances [5] by third parties [4]-[9]. This can be used to reconstruct the visual information and use the obtained data to compromise information security.

The main sources of CEE in CE video paths are the graphics adapter, interface cables, and monitor device controllers. CEE from the video path can be divided into two components [4]-[6], [10]. The first part includes components related to the clock signal (pixel frequency) of the video path, which determines the temporal structure of video data transmission. The second part contains information about the color components of the image and synchronization signals.

The conducted analysis [11]-[15] of traditional and new methods of protecting information from leakage through channels of side electromagnetic radiation of video paths of computing equipment shows that most existing approaches are focused on the general attenuation or masking of side-channel electromagnetic radiation without taking into account their spectral structure and the degree of information content of individual frequency components.

In a number of studies [2]-[10] using SDR [16] receivers and specialized software, visual information was reconstructed based on the analysis of CEE. A key feature of these approaches is that image reconstruction was performed exclusively at a single fixed frequency, without considering information components in other frequency ranges.

In [15], the author investigated the spectrum of CEE from computer systems video paths depending on monitor screen resolution and frame refresh rate. It was found that the spectral components of CEE from video paths are formed at multiples of the clock signal frequency.

In this regard, a pressing task is to determine the spectral frequency components of CEE from computer video paths, in terms of their information content for restoring visual information. This will further substantiate the selection and development of methods and technical protection measures aimed at selectively suppressing the most vulnerable frequency ranges and improving the effectiveness of visual information leakage prevention.

The following are this work's primary contributions:

An SDR receiver in a realistic electromagnetic environment is used in an experimental investigation of compromising electromagnetic emanations of computer video routes.

Reconstructing visual information is made possible by the identification of particular harmonic frequency components of the pixel clock signal.

Reconstructed images are compared using both quantitative similarity criteria and perceptual readability.

The practical informational readability of reconstructed images is shown to be not fully reflected by traditional pixel-wise similarity measurements.

A frequency-selective method for enhancing visual information security against electromagnetic leakage is justified.

2 METHODS

The methodological basis of the study is aimed at experimentally investigating the spectral components of stray electromagnetic emissions from computer video paths in terms of their informative value for visual information recovery. The approach is based on measuring electromagnetic emissions in the frequency domain and identifying potentially dangerous frequencies at which image reconstruction by computer systems is possible.

The experimental study involves several sequential stages. In the first stage, the clock (pixel) frequency of the video path of the computing system under study is determined.

In the second stage, the multiple harmonic components corresponding to this clock frequency are calculated. In the third stage, the levels of CEE from the computing system's video path are measured in the selected frequency ranges. In the fourth stage, visual information is reconstructed using the TempestSDR software based on the multiple harmonics of the CEE [17].

The experimental setup is used to receive stray electromagnetic emissions generated by the computer's video system while displaying images on the screen. The setup consists of a computer and monitor as the test object, a software-defined radio receiver (SDR) with a broadband antenna for receiving CEE signals, and a separate personal computer running TempestSDR software for reconstructing images from CEE.

Experimental conditions: The monitor's screen resolution was 1024×768, and the frame refresh rate was 75 Hz. A HackRF One device with an SA-7000 whip omnidirectional antenna was used as the SDR receiver. The distance between the monitored computer system and the receiving antenna was 1 m. This distance was selected to represent a realistic near-field eavesdropping scenario consistent with prior TEMPEST studies (e.g., adjacent-room or corridor interception), while remaining within the sensitivity range of the HackRF One/whip-antenna receiver used; signal levels are expected to decrease approximately with the inverse square of distance in the far field, so reconstruction at greater distances (e.g., several meters) would require either a higher-gain directional antenna or would be limited to the strongest harmonics identified in Table 2. Measurements were conducted in a realistic electromagnetic environment without additional shielding. Signal acquisition and image reconstruction were performed using the TempestSDR software. In the TempestSDR software, the reception bandwidth and sampling rate were configured to 20 MHz and 20 MS/s, respectively. For the discrete signal-level measurements reported in Table 1, the analysis (resolution) bandwidth of the spectral estimation was set to 10 kHz, matching the frequency resolution used to isolate each harmonic peak from the surrounding noise floor; this RBW setting was held constant across all measured harmonics to ensure comparability of the reported dBm values. Gain was set to automatic (AGC). After initiating the receiver, the center frequency was tuned sequentially to each target harmonic frequency, and the screen resolution (1024×768) and frame refresh rate (75 Hz) were set within the software to enable synchronization and image reconstruction. All receiver and reconstruction parameters were kept constant during the experiment to ensure reproducibility of the obtained results. The experimental schematic is shown below (Fig. 1).

To record the CEE signal level at the test object, a test pattern [18] was initiated, which increased the CEE signal level. Following the CEE level measurement at the test object, a test image is generated and displayed (Fig. 2), the CEE signals of which are then received and reconstructed. The test image includes symbolic, geometric, and color elements with distinct spatial boundaries, ensuring the sensitivity of the similarity metrics to distortions that occur during the interception and reconstruction of the video signal via the CEE channels.

All experiments were conducted on authorized equipment for defensive research purposes.

Measurements at each harmonic frequency were performed in five repeated trials under identical experimental conditions. The signal levels demonstrated stable and repeatable results with variations not exceeding ±0.3 dBm. All signal levels reported in Table 1 are the arithmetic mean of the five trials; the observed inter-trial standard deviation did not exceed 0.15 dBm at any harmonic (the ±0.3 dBm figure above reflects the maximum peak-to-peak spread across trials, i.e., approximately 2 standard deviations), indicating good measurement repeatability under the fixed instrument configuration used throughout the study.

3 RESEARCH RESULTS

Since the screen resolution is standard: 1024x768 and the frame refresh rate is 75 Hz, we can calculate the clock signal frequency using the formula given in the work [15] or find it in the document [19]. The clock signal frequency is 78.750 MHz. The clock signal's multiple harmonics are calculated using the formula (1).

$$F_n = n \cdot f_p, \tag{1}$$

where: f_p - pixel clock frequency (MHz); n - harmonic number *(n = 1, 2, 3, ...);* F_n - frequency of the nth harmonic (MHz).

The results of harmonic calculations and CEE level measurements are presented in Table 1.

Using the data presented in Table 1, an attempt was made to recover visual information from the stray electromagnetic emissions of the computer system's video path using the TempestSDR software and the HackRF One software-defined radio receiver. Image reconstruction was not possible at all frequencies studied.

Table 2 presents the results, reflecting the frequencies at which image reconstruction was possible. Each harmonic frequency was measured in multiple trials, and the obtained signal levels and reconstructed images demonstrated stable and repeatable results.

Where:

- "+" - Detectable informative content;
- "-" - No detectable informative content.

Below in Figure 3-6 the results of reconstructed images from CEE are presented.

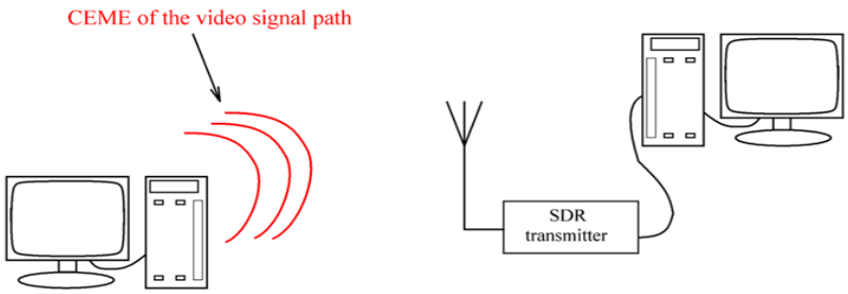

Figure 1: Structural diagram of the experiment.

Figure 2: Test image.

Table 1: Measured harmonic frequencies and corresponding CEE signal levels.

Harmonic number	1	2	3	4	5	6	7	8	9	10
Frequencies, MHz	78.750	157.5	236.25	315	393.75	472.5	551.25	630	708.75	787.5
Signal Level, dBm	-70.5	-71.3	-72.1	-72.9	-73.5	-74.9	-75.8	-77.1	-78.2	-78.9

Table 2: Image reconstruction capability at different harmonic frequencies.

Harmonic number	1	2	3	4	5	6	7	8	9	10
Frequencies, MHz	78.750	157.5	236.25	315	393.75	472.5	551.25	630	708.75	787.5
Possibility of recovery	-	-	-	-	+	+	+	-	+	-

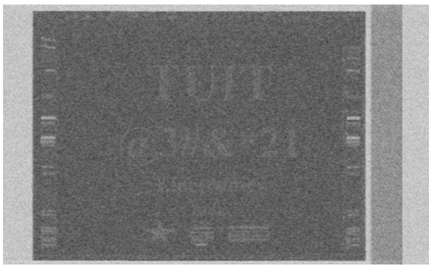

Figure 3: Intercepted and reconstructed image at the 5th harmonic (393.75 MHz).

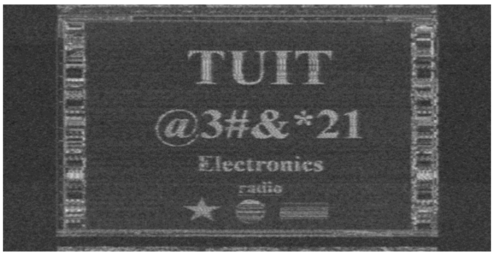

Figure 4: Intercepted and reconstructed image at the 6th harmonic (472.5 MHz).

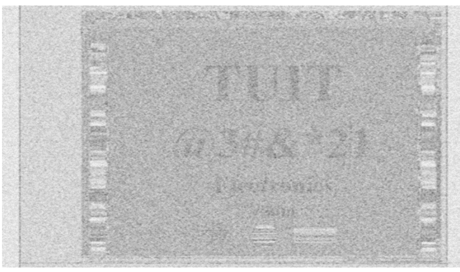

Figure 5: Intercepted and reconstructed image at the 7th harmonic (551.25 MHz).

Figure 6: Intercepted and reconstructed image at the 9th harmonic (708.75 MHz).

Among the four reconstructed images (video frames) shown in Figures 3–6, the image reconstructed at 472.5 MHz (Fig. 4) exhibits the highest degree of similarity to the original video frame in terms of visual information content, structural characteristics, and overall perceptual quality. This indicates that the corresponding harmonic carries more recoverable visual information than the other frequencies investigated.

To complement the visual analysis, objective image similarity metrics, namely the Peak Signal-to-Noise Ratio (PSNR) and Structural Similarity Index Measure (SSIM), were calculated between the original image and each reconstructed image [20]–[22]. The obtained values are summarized in Table 3. Although these metrics provide a quantitative measure of image similarity, they do not fully reflect the perceptual readability of the reconstructed images. This discrepancy may be attributed to the sensitivity of PSNR and SSIM to pixel-level noise and global brightness variations rather than to the preservation of structural and semantic information. At 472.5 MHz, the reconstructed image retains perceptually important features, such as text and geometric boundaries, that remain recognizable to a human observer despite higher noise levels, which reduce the numerical values of pixel-based similarity metrics. A comprehensive evaluation of the applicability and limitations of quantitative image similarity metrics for assessing electromagnetic information leakage is beyond the scope of the present study and will be addressed in future work.

Table 3: Objective similarity metrics for reconstructed images.

Frequency (MHz)	PSNR (dB)	SSIM
393.75	5.82	0.109
472.5	4.08	0.098
551.25	10.05	0.105
708.75	8.75	0.099

Although higher PSNR and SSIM values are observed at certain harmonic frequencies, visual analysis indicates that the reconstruction at 472.5 MHz provides greater informational readability for human perception. This demonstrates that conventional pixel-wise similarity metrics should be regarded as auxiliary indicators rather than decisive criteria in the assessment of electromagnetic information leakage. A more comprehensive analysis of quantitative similarity metrics in the context of electromagnetic image reconstruction will be addressed in future research. The mismatch at 472.5 MHz (PSNR = 4.08 dB, SSIM = 0.098, yet visually recognizable content) can be explained by the sensitivity of pixel-wise metrics to global geometric misalignment: TempestSDR reconstruction is prone to small residual timing offsets, sub-pixel horizontal shear, and brightness/contrast scaling relative to the reference source image, all of which strongly penalize PSNR and SSIM (which compare pixel intensities at fixed spatial coordinates) even when the underlying structural content, such as text blocks, window outlines, and image layout, remains clearly legible to a human observer. This suggests that alignment-tolerant or perceptual metrics (e.g., feature-based similarity, mutual information, or human-subject legibility scoring) would likely be more appropriate for this task than strict pixel-wise PSNR/SSIM, and their adoption is recommended for future work.

As shown in Table 2, the ability to reconstruct visual information from CEE from the computer system's video path is selective and is observed only at individual harmonic components of the clock signal. Specifically, successful image reconstruction was recorded at frequencies corresponding to the 5th, 6th, 7th, and 9th harmonics, while at the remaining harmonics, reconstruction was difficult or impossible. This result confirms the uneven distribution of CEE information components across the spectrum and points to the presence of a limited set of vulnerable frequencies that are of greatest interest for both interception and the development of selective suppression methods for information security applications. Notably, reconstruction success does not track signal amplitude alone: the 9th harmonic (−78.2 dBm) supports reconstruction despite being among the weakest measured levels, while the stronger 8th harmonic (630 MHz, −77.1 dBm) does not. This indicates that raw signal strength in Table 1 is not by itself a reliable predictor of reconstructability, and that other factors specific to each harmonic likely govern outcome, most plausibly (i) the local RF interference environment at each specific frequency (e.g., co-channel broadcast, Wi-Fi, or other ambient emitters that raise the effective noise floor independently of the CEE signal level), (ii) frequency-dependent antenna gain and impedance matching of the whip antenna, which is not flat across the measured band, and (iii) phase coherence and timing-recovery stability of the TempestSDR synchronization loop at each specific harmonic, which affects reconstruction quality independently of raw power. Distinguishing among these candidate explanations would require additional measurements (e.g., a controlled anechoic-chamber comparison or antenna gain calibration across the band) that fall outside the scope of the present study.

4 DISCUSSION

The study confirms that the information components of CEE from computer system video paths are distributed unevenly across the spectrum and are concentrated primarily in a limited set of frequencies corresponding to individual clock signal harmonics. This is consistent with the physical nature of CEE formation, in which the temporal structure of the video signal and the encoding processes of digital interfaces have a decisive influence on the spectral density of the emissions.

These results demonstrate that using a single fixed frequency to assess video path vulnerability does not adequately characterize the actual threat level of visual information leakage. Analysis of the spectral components of CEE from computer system video paths allows us to identify the most vulnerable frequencies at which stable restoration of visual information is ensured. This finding extends the classical TEMPEST literature, which historically assessed video-path emanation risk primarily at a single fixed frequency, typically the fundamental pixel-clock frequency or its immediately adjacent harmonics, as in the foundational work of van Eck and the later systematic treatment by Kuhn [2]. By systematically sweeping and comparing multiple harmonics rather than assuming the strongest or lowest-order harmonic is necessarily the most exploitable, the present multi-harmonic approach reveals that reconstructability is harmonic-specific and non-monotonic in signal strength (Table 2), a distinction that a single-frequency assessment methodology would not have captured and that has direct implications for designing selective, frequency-targeted shielding rather than broadband suppression.

From a practical standpoint, this creates the preconditions for a transition from broadband protection methods, such as general noise suppression or shielding, to selective approaches aimed at suppressing specific information-rich spectral components. This approach improves protection efficiency while reducing energy costs and the negative impact on the electromagnetic compatibility of computing systems.

5 CONCLUSIONS

The study demonstrates that visual information recovery from CEE from video paths is only possible within a limited set of frequency components associated with specific clock signal harmonics. The experimental results confirm the uneven spectral distribution of information-rich emissions and indicate the presence of specific vulnerable frequency regions.

The similarity between the original and reconstructed images was evaluated both visually and using objective similarity metrics (PSNR and SSIM). The results indicate that quantitative similarity measures do not always fully correspond to perceptual informational readability. This confirms the importance of combining visual and metric-based analysis when assessing the risk of electromagnetic information leakage.

The proposed frequency-based analysis provides a methodological basis for developing selective protection methods aimed at suppressing the most informative spectral components, rather than relying on broadband countermeasures. This approach improves the effectiveness of visual information leakage prevention while simultaneously reducing excess electromagnetic interference and maintaining system performance.

REFERENCES

[1] T. Liu and Y. Li, Electromagnetic Information Leakage and Countermeasure Technique. Cham, Switzerland: Springer, 2019.

[2] M. G. Kuhn, "Electromagnetic eavesdropping risks of flat-panel displays," in Proc. 4th Int. Workshop Privacy Enhancing Technol. (PET), Toronto, Canada, May 2005, pp. 88-107.

[3] M. Martin, F. Sunmola, and D. Lauder, "Likelihood of unintentional electromagnetic emanations compromising IT equipment security: Perspectives of practitioners on causal factors," in Proc. 2021 Int. Carnahan Conf. Security Technol. (ICCST), Hatfield, United Kingdom, 2021, pp. 1-6, [Online]. Available: https://doi.org/10.1109/ICCST49569.2021.9717369.

[4] D.-H. Choi, E. Lee, and J.-G. Yook, "Reconstruction of video information through leakaged electromagnetic waves from two VDUs using a narrow band-pass filter," IEEE Access, vol. 10, pp. 40307-40315, 2022, [Online]. Available: https://doi.org/10.1109/ACCESS.2022.3162686.

[5] P. de Meulemeester, B. Scheers, and G. A. E. Vandenbosch, "Eavesdropping a (ultra-)high-definition video display from an 80 meter distance under realistic circumstances," in Proc. 2020 IEEE Int. Symp. Electromagn. Compat. Signal/Power Integrity (EMCSI), Reno, NV, USA, 2020, pp. 517-522, [Online]. Available: https://doi.org/10.1109/EMCSI38923.2020.9191457.

[6] P. De Meulemeester, B. Scheers, and G . A. E. Vandenbosch, "A quantitative approach to eavesdrop video display systems exploiting multiple electromagnetic leakage channels," IEEE Trans. Electromagn. Compat., vol. 62, no. 3, pp. 663-672, Jun. 2020, [Online]. Available: https://doi.org/10.1109/TEMC.2019.2923026.

[7] W. Huang, Z. Feng, and Y. Xu, "Analysis on the modeling and image restoration of electromagnetic radiation leakage," in Proc. 2021 IEEE 6th Int. Conf. Signal Image Process. (ICSIP), Nanjing, China, 2021, pp. 516-520, [Online]. Available: https://doi.org/10.1109/ICSIP52628.2021.9688726.

[8] I. Kubiak, "Digital processing methods of images and signals in electromagnetic infiltration process," Image Process. Commun., vol. 18, no. 1, pp. 5-14, 2013, [Online]. Available: https://doi.org/10.2478/v10248-012-0070-7.

[9] E. Lee, D.-H. Choi, T. Nam, and J.-G. Yook, "A quantitative analysis of compromising emanation from TMDS interface and possibility of sensitive information leakage," IEEE Access, vol. 10, pp. 73997-74011, 2022, [Online]. Available: https://doi.org/10.1109/ACCESS.2022.3184294.

[10] T. Kitazawa, S. Matsumoto, and Y. Hayashi, "Pixel level character reconstruction by background profiling against TMDS emanations," in Proc. 2025 IEEE Int. Symp. Electromagn. Compat., Signal Power Integrity (EMC+SIPI), Raleigh, NC, USA, 2025, pp. 60-65, [Online]. Available: https://doi.org/10.1109/EMCSIPI52291.2025.11170210.

[11] M. Bugaj, R. Przesmycki, L. Nowosielski, and K. Piwowarczyk, "Techniques shielding of objects with to compromising emanations," in Proc. 2012 19th Int. Conf. Microwaves, Radar Wireless Commun. (MIKON), Warsaw, Poland, 2012, pp. 559-562, [Online]. Available: https://doi.org/10.1109/MIKON.2012.6233566.

[12] K. Foziljonov and I. Faziljanov, "Active methods and means of information protection against leakage through channels of side electromagnetic radiation and interference," Science and Innovation, vol. 2, no. A4, pp. 46-52, 2023, [Online]. Available: https://doi.org/10.5281/zenodo.7818479, [Accessed: Feb. 23, 2026].

[13] R. Lavaud, R. Gerzaguet, M. Gautier et al., "Whispering devices: A survey on how side-channels lead to compromised information," J. Hardw. Syst. Secur., vol. 5, pp. 143-168, 2021, [Online]. Available: https://doi.org/10.1007/s41635-021-00112-6.

[14] M. Guri and Y. Elovici, "Bridgeware: The air-gap malware," Commun. ACM, vol. 61, no. 4, pp. 74-82, Apr. 2018, [Online]. Available: https://doi.org/10.1145/3177230.

[15] F. K. I. Ogli, "Study of the spectrum of side electromagnetic radiations of video interface DVI," in Proc. 2021 Int. Conf. Inf. Sci. Commun. Technol. (ICISCT), Tashkent, Uzbekistan, 2021, pp. 1-3, [Online]. Available: https://doi.org/10.1109/ICISCT52966.2021.9670090.

[16] S. Fernández, F. Paez, G. Varela, L. Belzner, and P. Gimenez, "Deep-TEMPEST: Using deep learning to eavesdrop on HDMI from its unintended electromagnetic emanations," arXiv preprint arXiv:2407.09717, Jul. 2024, [Online]. Available: https://arxiv.org/abs/2407.09717, [Accessed: Feb. 23, 2026].

[17] E. Thiele, "TempestSDR," GitHub repository, [Online]. Available: https://github.com/eried/Research/tree/master/HackRF/TempestSDR, [Accessed: Feb. 11, 2024].

[18] E. Thiele, "Tempest for Eliza," [Online]. Available: http://www.erikyyy.de/tempest/, [Accessed: Feb. 12, 2024].

[19] VESA, Video Electronics Standards Association Display Monitor Timing (DMT) Standard, Version 1, Revision 11. Milpitas, CA, USA: VESA, 2007.

[20] A. Horé and D. Ziou, "Image quality metrics: PSNR vs. SSIM," in Proc. 2010 20th Int. Conf. Pattern Recognit. (ICPR), Istanbul, Turkey, 2010, pp. 2366-2369, [Online]. Available: https://doi.org/10.1109/ICPR.2010.579.

[21] T. Nam, D.-H. Choi, E. Lee, H.-S. Jo, and J.-G. Yook, "Data generation and augmentation method for deep learning-based VDU leakage signal restoration algorithm," IEEE Trans. Inf. Forensics Security, vol. 19, pp. 5220-5234, 2024, [Online]. Available: https://doi.org/10.1109/TIFS.2024.3393748.

[22] A. M. Vizitiu, C. Niţă, I. Ţigănescu, and C. Lungoci, "Comparative approach to de-noising TEMPEST video frames," Sensors, vol. 24, no. 19, p. 6292, Sep. 2024, [Online]. Available: https://doi.org/10.3390/s24196292.